eprints@whiterose.ac.uk
https://eprints.whiterose.ac.uk/

Optimal PV cell coverage ratio for semi-transparent photovoltaics on office building façades in central China

Shen Xu [a,b], Wei Liao [b], Jing Huang [b], Jian Kang [a,*]

[a]School of Architecture, University of Sheffield, Arts Tower, Western Bank, Sheffield, S10 2TN, UK

[b]School of Architecture and Urban Planning, Huazhong University of Science and Technology, 1037 Luoyu Road, Wuhan, China

*Corresponding author: j.kang@sheffield.ac.uk

Abstract:

   The present study investigates the optimal PV cell coverage ratio in terms of the overall energy consumption of office buildings in central China for which semi-transparent photovoltaic façades have been implemented, with various combinations of architectural variables including room depth, window-to-wall ratio (WWR), and orientation. Here, models and methods are established for the calculation of PV cell coverage ratio for a single-glazed semi-transparent PV façade and these models and methods are validated through field experiments. The established techniques are then incorporated into Energy Plus to perform a parametric analysis of the effects of different PV cell coverage ratios on overall energy consumption. The results show that PV cell coverage ratio has a pronounced effect on electricity consumption and that its impact is influenced by different combinations of room depth, WWR, and orientation. Moreover, the selection of an optimal PV cell coverage ratio is found to be an important element of the design approach in building-integrated PV (BIPV) systems: use of the optimal PV cell coverage ratio can achieve overall energy consumption savings of 13% (on average) compared to the least favourable PV cell coverage ratio.

Keywords: optimal PV cell coverage ratio, semi-transparent PV, office building façade, overall energy consumption

1. Introduction

   In recent years, interest in low-carbon development and renewable energy applications in buildings has increased considerably [1]. In particular, building-integrated photovoltaic (BIPV) technology is becoming widely used in parts of the façades of modern buildings [2-5]. Office buildings are particularly suitable for BIPV as they consume energy primarily in daytime, which is when the PV system collects and converts solar energy into electricity; thus, the effort and cost associated with energy storage can be avoided [6]. Such PV

façades are being used increasingly in office building designs in China [7]. Accordingly, the development of an optimal PV façade design for architects, constructors, and installers is becoming increasingly urgent.

Semi-transparent PV technology is known to be beneficial for office buildings in terms of overall energy savings. For example, semi-transparent photovoltaics not only generate electricity, but also introduce daylight that can reduce artificial lighting energy consumption in daytime [8]. Conversely, semi-transparent photovoltaics reduce heat gain by blocking incoming solar radiation with PV cells [9], which increases heating demand indoors in winter but reduces the cooling demand in summer.

The transmittance of PV panels or glass for PV façades, which is determined by the PV cell coverage ratio, has been shown to have a profound impact on the overall energy consumption of buildings, particularly through its effects on PV electricity generation, lighting, cooling, and heating [10-12]. For example, Jiang et al. [10] conducted a study to investigate the influence of PV cell coverage ratio on the thermal and electrical performance of photovoltaic Trombe walls and discovered that a higher PV cell coverage ratio does not necessarily result in better thermal performance. In terms of overall energy consumption, Wong et al. [11] described the minimisation of energy consumption based on combinations of semi-transparent PV transmittance and window-to-wall ratios (WWRs). Conversely, Miyazaki et al. [12] found lighting control to be an important element in maximising the usage of daylight and demonstrated that the impact of solar cell transmittance on energy performance varied with WWR. In general, PV cell coverage ratio controls the transmittance of semi-transparent PV façades and the studies described above suggest the existence of an optimal PV cell coverage ratio that can achieve the minimum overall energy consumption. However, Yun et al. [13] found that adopting a certain range of WWR and room depth could maximise the benefits of a ventilated PV façade; this suggests that the optimal PV cell coverage ratio must be determined under different combinations of architectural factors to ensure that the best energy performance is achieved.

The overall energy-saving effects of semi-transparent PV windows appear to vary with climate. In Brazil, the use of a semi-transparent PV window has been shown to save up to 43% of energy [14]. Conversely, in Japan, 55% energy savings were achieved (compared to a single-glazed window) with a solar cell transmittance of 40% and WWR of 50% [12], whereas energy savings of 16.7–41.3% were achieved in Singapore for a WWR range of 70–100% [15]. Other previous studies [16-17] have also demonstrated the importance of considering climatic conditions in the investigation of semi-transparent PV window applications. However, few studies to date have attempted a comprehensive determination of optimal PV cell coverage ratio for semi-transparent PV technology using different combinations of architectural factors such as room depth, WWR, and orientation. Accordingly, no general trends have been defined regarding variations in optimal PV cell coverage ratio. Such knowledge will play a crucial role in future optimal design approaches for semi-transparent PV façades, and improvements in the understanding of the variation in PV cell coverage ratio are required urgently. In particular, previous studies providing accurate assessments of the overall energy performance of semi-transparent PV façades in China are extremely limited, and few relevant experiments have been conducted under climatic conditions such as those in central China. Studies conducted under real climatic conditions are necessary because several studies investigating semi-transparent PV in different climate zones have produced different results.

The present study aims primarily to improve the determination of optimal PV cell coverage ratio, to understand trends in the variation of optimal PV cell coverage ratio with different architectural conditions, and to investigate the impact of architectural conditions on overall energy consumption. Additionally, it is hoped that the results presented here will provide a general reference point for the incorporation of optimal PV cell coverage ratio into the design approach as an important element necessary for the implementation of

semi-transparent PV technology in office buildings. This should help to maximise the benefits of semi-transparent PV usage in office buildings, particularly in central China. In this paper, the methodology adopted for the present study (including field experiments, architectural models, and calculation models and methods) is first described. Then, the results are presented in terms of the different effects of PV cell coverage ratio on lighting, cooling, and heating energy consumption. Finally, the determination of optimal PV cell coverage ratio is described and the variation in optimal PV cell coverage ratio with variations in room depth, WWR, and orientation is discussed.

2. Methodology

In the present study, models and methods for the calculation of PV cell coverage ratio in relation to semi-transparent PV technology were established and validated based on field experiments in Wuhan, which can be considered representative of the climatic conditions of central China. The field experiments also provided more accurate data regarding the properties of semi-transparent PV glasses. An architectural model was developed with a series of generic office rooms. In these rooms, architectural characteristics including room depth, WWR, and orientation were incorporated in different combinations to allow evaluation of the effects of PV cell coverage ratio under different architectural conditions. Finally, the architectural model and validated models and methods were used in computational simulations with Energy Plus. In this manner, a parametric analysis was conducted to evaluate the effects of PV cell coverage ratio on electricity consumption under different architectural conditions.

2.1. Experimental set up

The experiments were conducted in an experimental room built on the roof of a building in Wuhan (29°58′N, 113°53′E). The experimental room had length, width, and height of 4.65 m, 3.4 m, and 3.6 m, respectively, and was constructed using mineral wool board with a thickness of 12 mm as thermal insulation wall. The experimental room contained two inner chambers sharing a guarded room, each of which included a window that was 1.1 m long and 1.3 m high on the southern façade. A photo of the experiment room is shown in Fig. 1.

The field experiment was conducted 24 h a day from June 2012 to August 2013. The temperature on both sides of the PV glass was recorded with several T-type thermocouples at the surface of the glass. These thermocouples have been calibrated by placing them, together with a standard mercury thermometer (with precision of 0.1°C), into a thermostatic water bath with temperature ranging from 0°C to 100°C. Through this calibration, the accuracy of the thermocouples was improved to ±0.1°C, which meets the test requirements. The vertical solar irradiance of the southern orientation was recorded with a pyranometer device of Jinzhou Sunshine TBQ-2 set at the southern wall. The pyranometer device

Fig. 1 Photo of the experimental room

was calibrated by the manufacturer before the experiments. The PV electricity generation of each PV glass was recorded every minute throughout the test period. Because the maximum power varied according to the solar irradiance and the maximum power point changed constantly, MPPT (maximum power point tracking) systems were used to detect the maximum power point of PV electricity generation. General data describing weather conditions were recorded at hourly intervals with the Davis Vantage Pro 2 weather station. Solar irradiance, temperature, and PV electricity generation data were collected using the Agilent 34972A data logger and sent to a central computer for storage.

2.2. Calculation models and methods for semi-transparent PV

2.2.1 Power generation

PV power generation efficiency is affected by the temperature of solar cells, such that PV efficiency decreases with increasing temperature [18]. Moreover, a PV panel with high PV cell coverage ratio will absorb more solar radiation (and thus achieve a higher temperature) than a panel with low PV cell coverage ratio; this produces inconsistent results in terms of PV power generation efficiency, even under the same climatic conditions [10]. To address this, a temperature coefficient power generation model [19] must be included.

$$P = G\,\eta_{\mathrm{O}}[1 - \beta_{\mathrm{C}}(T_{\mathrm{c}} - 25^{\circ}\mathrm{C})] \tag{1}$$

where P is the instant power of the PV panel, G is solar radiation on the PV plane (W/m^2), η_{o} is PV efficiency under standard conditions, β_{C} is the temperature coefficient, and T_{c} is the solar cell temperature (°C), which will be affected by PV cell coverage ratio. In this model, the solar cell temperature T_{c} is unknown and must be provided using heat balance models (as described in Section 2.2.2). In the present study, the temperature coefficient β_{C} was determined to be -0.72%/°C based on field experiments.

The results obtained using the power generation model were compared with measurements obtained during field experiments. It was demonstrated that the power generation model can predict PV electricity output with satisfactory accuracy. For example, Fig. 2 compares the measured and calculated PV electricity output results for a semi-transparent PV panel with PV cell coverage ratio of 40% using the climate data obtained for August 1 2013 and clearly indicates good agreement, with an average deviation of 7.5%. Other comparisons in all four seasons were also made; the results show good agreement, with less than 9.2% deviation in all cases.

2.2.2 Heat balance model

The temperature of the solar cell layers of semi-transparent PV panels must be calculated using a heat balance model. Single-glazing semi-transparent PV glass consists of multiple layers of materials, including internal and external layers of clear glass (each 6 mm thick) with a central layer of EVA that contains a silicon cell of different PV cell coverage ratio. In the heat balance model adopted here, the semi-transparent PV glass is divided into 3 layers with 4 boundaries. The properties of each layer are provided by the manufacturer and are presented in Table 1. The temperature of each boundary was calculated based on heat balance equations. The

4

temperature of the solar cell layer T_c was assumed to be the average of T_2 and T_3 because the difference between these two values was negligible in the context of the model outcome. Heat storage in the single glazing was not considered and heat transfer was assumed to be in quasi-steady state. Thus, the heat balance equations for the first, second, third, and fourth boundaries were established as in Eqs. (2), (3), (4), and (5), respectively.

$$G\alpha_1 = (T_1 - T_{out})h_{out,c} + \xi\sigma\left[(T_1 - 273.15)^4 + (T_{out} - 273.15)^4\right] + \frac{\lambda_1}{d_1}(T_1 - T_2) \tag{2}$$

$$G\tau_1\left[(1-PVR)\alpha_{EVA} + PVR\alpha_{sc}\right] + \frac{\lambda_1}{d_1}(T_1 - T_2) = \frac{\lambda_2}{d_2}(T_2 - T_3) + P \tag{3}$$

$$G\tau_1(1-PVR)\tau_{EVA}\alpha_3 + \frac{\lambda_2}{d_2}(T_2 - T_3) = \frac{\lambda_3}{d_3}(T_3 - T_4) \tag{4}$$

$$\frac{\lambda_3}{d_3}(T_3 - T_4) = h_{in,c}(T_4 - T_{in}) + \xi\sigma\left[(T_4 + 273.15)^4 - (T_{in} + 273.15)^4\right] \tag{5}$$

where G is solar radiation on the PV plane (W/m^2), α_i is the solar absorptance of layer i, and T_i is the temperature of boundary i. Additionally, T_{out} and T_{in} are the outdoor and indoor temperatures, respectively; $h_{out,c}$ and $h_{in,c}$ are the convective heat transfer coefficients for the outside and inside surfaces, respectively, of the semi-transparent PV panel; ξ is the emissivity of the front glass; σ is the Stefan–Boltzmann constant (W/m^{2}K^4); τ_i is the solar transmittance of layer i; *PV cell coverage ratio* is the solar cell coverage ratio; λ_i is the heat conductivity of layer i (W/mK); λ_{sc} and λ_{EVA} are the heat conductivity of the solar cell and EVA, respectively (W/mK); P is the PV power generation (W/m^2); and d_i is the thickness of layer i (m). The external and internal surface convection heat transfer coefficients were set to 16 W/m^{2}K and 3.6 W/m^{2}K, respectively, based on data obtained from the standard entitled 'Calculation specification for thermal performance of windows, doors and glass curtain-walls' (JGJ/T 151-2008) [20].

The results calculated from the heat balance model were compared with the measurements collected during field experiments. Figure 3 illustrates variations in the inside surface temperature of a semi-transparent PV panel with PV cell coverage ratio of 40% throughout the course of a day (March 1 2013) and demonstrates clearly that the calculated results agree well with the measurements, with less than 0.61°C deviation. Other comparisons in all four seasons were also made; the results show good agreement, with an average deviation of less than 1.1°C in all cases.

To calculate the heat and solar radiation transfer, which affects the heating and cooling loads of the indoor space, it is necessary to obtain the U-factors and solar heat gain coefficients (SHGCs) for the different PV cell coverage ratio glasses studied [20]. SHGCs can be calculated according to Eq. (6):

$$SHGC = \tau + N\alpha \tag{6}$$

where τ is total solar transmittance of semi-transparent photovoltaics, N is the inward-flowing fraction of the absorbed radiation, and α is the total solar absorptance of semi-transparent photovoltaics with different PV cell coverage ratio and can be obtained from WINDOW 6.3 using the properties presented in Table 1. Furthermore, τ and N can be defined as in Eqs. (7) and (8), respectively.

$$\tau = \tau_1 \tau_2 \tau_3 (1 - PVR) \tag{7}$$

$$N = \frac{h_{in}}{h_{in} + h_{out}} \tag{8}$$

where h_{out} and h_{in} are outside and inside heat transfer coefficients, respectively, for the surfaces of semi-transparent PV panels. Similarly, U-factors can be calculated for different PV cell coverage ratio as follows:

$$U = \frac{1}{\dfrac{1}{h_{out}} + \dfrac{d_1}{\lambda_1} + \dfrac{d_2}{\lambda_2} + \dfrac{d_3}{\lambda_3} + \dfrac{1}{h_{in}}} \tag{10}$$

In the present study, the outside and inside surface heat transfer coefficients were set to 20.2 W/m²K and 8.3 W/m²K, respectively, based on data obtained from the standard entitled 'Calculation specification for thermal performance of windows, doors and glass curtain-walls' (JGJ/T 151-2008) [20]. After calculation of SHGCs and U-factors, heating and cooling loads were simulated in Energy Plus.

Table 1 Properties of individual layers of PV cells

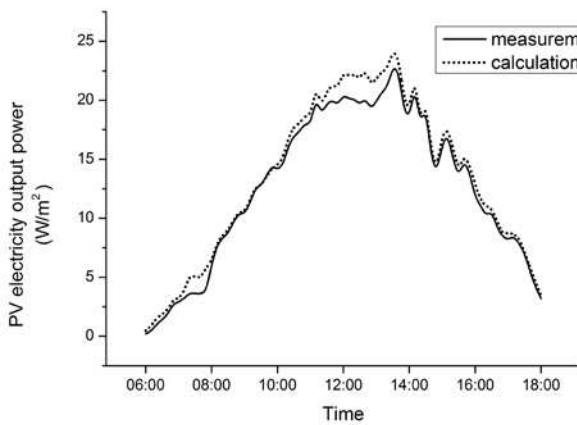| layer	thickness (mm)	thermal conductivity (W/mK)	absorptance	transmittance	reflectance
glass	6	0.760	0.108	0.810	0.082
EVA	1.8	0.116	0.060	0.900	0.040
silicon cell	0.3	168.0	0.970	0	0.030

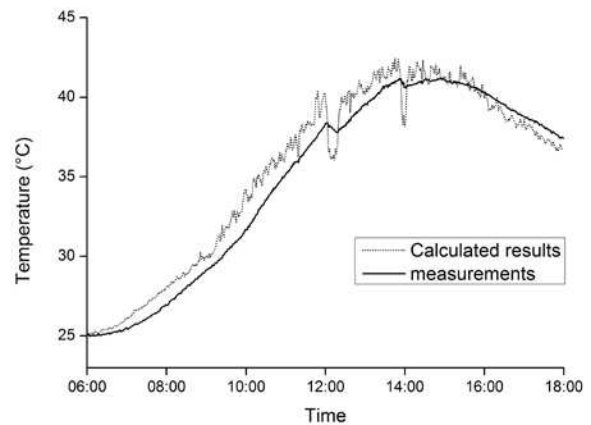Fig. 2 Comparison of measured and calculated PV electricity output power

Fig. 3 Comparison of observed and simulated inside surface temperatures for single-glazed semi-transparent PV panels

2.2.3 Daylight and lighting control

According to the Standard for Lighting Design of Buildings for China (GB50034-2004) [21], indoor illuminance should reach 300 lux in general office rooms. To simulate such conditions and incorporate the energy savings achieved during daylight, daylight detection and lighting control were introduced into the simulation with the help of Energy Plus. When the daylight illuminance level fell below 300 lux, artificial lighting was initiated to achieve the required illuminance level; however, this resulted in extra electricity consumption. Therefore, to obtain an accurate simulation outcome, visible transmittance was obtained from WINDOW 6.3 for each semi-transparent PV panel with different PV cell coverage ratio and was incorporated into Energy Plus as part of the daylight simulation. Thus, daylight illuminance was calculated and recorded in Energy Plus, allowing the simulation and calculation of lighting energy consumption [11].

2.3. Architectural model

An architectural model is a crucial part of the investigation of the energy performance of semi-transparent photovoltaics in office façades. To develop such a model, information was obtained by conducting a survey of 60 office building cases in the Wuhan area. Two typical types of office building were identified in the survey: buildings with core tubes and slab-type buildings. The division of large rooms into separate smaller rooms was found to be common in both types of office building; in fact, the majority of cases investigated exhibited such division. Thus, these separate rooms were incorporated into the models described here and used to represent the generic office rooms of the present study.

These generic office rooms were set to allow control of three main variables: (1) room depth, as shown in Fig. 4(a); (2) WWR, as shown as Fig. 4(b); and (3) orientation. By adopting various combinations of these variables, different PV cell coverage ratio could be examined under different architectural conditions, as shown in Fig. 4(c). Room depth was varied from 4 m to 13 m at intervals of 1 m; this range can be considered representative of common office room sizes in the Wuhan area. WWR was restricted to the range 0.2−0.7 based on guidelines presented in the Design Standard for Energy Efficiency of Public Buildings proposed by the Ministry of Housing and Urban–Rural Development of the PRC [22], which forbids office buildings with a WWR over 0.7 in the hot summer/cold winter climate zone [22]. PV cell coverage ratio was varied from 10% to 80% at intervals of 5%. PV cell coverage ratio lower than 10% would make PV applications uneconomical; conversely, PV cell coverage ratio higher than 80% would block the entire window area, making it difficult for daylight to enter the room and for occupants to see out. The adopted PV cell coverage ratio interval of 5% should allow a distinction to be made between the different impacts of PV cell coverage ratio while still remaining sufficiently practical for the simulation parametric analysis to be conducted.

Other simulation features required were assumed to be fixed and were based on the Design Standard for Energy Efficiency of Public Buildings for China [22], as follows. (1) A rectangular office room on an intermediate floor was assumed to have width and height of 5 m and 4 m, respectively. (2) The thermal properties of exterior and interior walls and ceilings and floors were as detailed in Table 2. (3) A single window area with no sun blinds was assumed, since the semi-transparent PV model serves as a shading device. (4) Room lights were assigned a design value of 11 W/m^2 in all instances. The daylight control sensor was located in the geometric center of the room at a height of 0.75 m. Daylight control initiated artificial lighting when the indoor illuminance level fell below 300 lux. (5) The daily heating and cooling schedules assigned for the air conditioning are presented in Table 3. COP was set to 4.5 and the ventilation system was set to ensure 1.5 air

changes/h. (6) Office occupancy was set to 0.25 people/m^2 and the electricity consumption of the equipment was assumed to be 20 W/m^2. (7) Lighting and office equipment operation schedules were set according to the office occupancy conditions presented in Table 3.
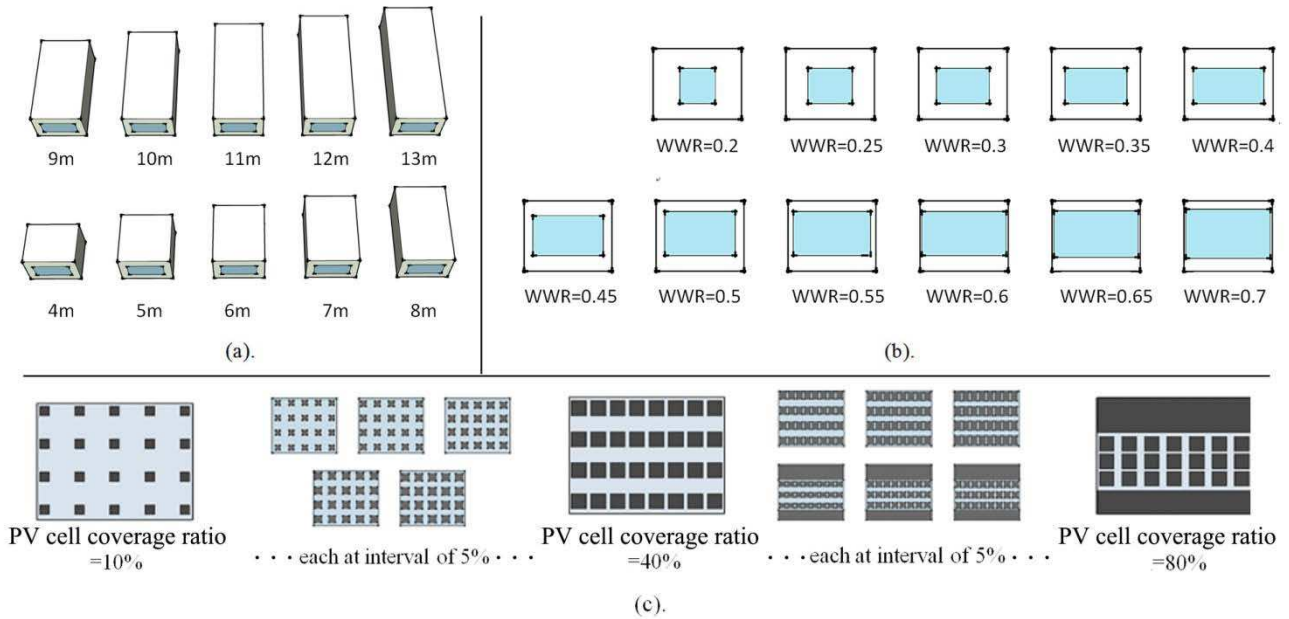

Fig. 4 Illustrations of variations in (a) room depth, (b) WWR, and (c) PV cell coverage ratio

Table 2 Thermal and optical properties of building layers

layer	thickness (mm)	thermal conductivity (W/mK)	density (kg/m^3)	specific heat (J/kg K)
exterior wall				
brick	200	0.89	1920	790
insulation board	40	0.03	50	1210
surface finish*2	20	0.16	800	1100
interior wall				
brick	100	0.89	1920	790
surface finish*2	20	0.16	800	1100
ceiling/floor				
standard wood board	8	0.12	540	1210
cast concrete	120	1.60	2200	860
surface finish	20	0.16	800	1100

Table 3 Hourly heating and cooling schedules

	time				
	00:00−07:00	07:00−08:00	08:00−17:00	17:00−19:00	19:00−24:00
cooling system (℃)	37	28	26	26	37
heating system (℃)	12	18	20	20	12
lighting, equipment, operation schedules (fraction of full operation)	0	0.5	0.95	0.3	0

8

3. Results and discussion

This section provides a discussion of the parametric analysis conducted. The validated calculation models and methods were incorporated into the architectural model defined above to investigate the effects of different PV cell coverage ratio on energy performance using Energy Plus. The overall energy performance, including PV electricity generation and lighting and heating and cooling electricity consumption, was examined under different architectural conditions. Different combinations of room depth and WWR were examined carefully for a southern orientation while PV cell coverage ratio was varied from 10% to 80% at 5% intervals. The criterion of electricity consumption per floor area (kWh/m^2) was used to account for differences in floor area for different values of room depth, thus providing normalised results. Other orientations are discussed in Section 3.4. All figures were evaluated based on annual or average annual values to ensure a holistic view of overall energy consumption with the consideration of all four seasons.

3.1 Effects on PV electricity generation

Solar cells convert solar energy into electricity and typically operate with a specific conversion efficiency, which is affected primarily by the material characteristics and operating temperature of the cells. Compared to transparent glass, silicon solar cells typically have higher solar absorbance. Thus, the amount of solar heat gained can be increased by adopting a denser solar cell array and, therefore, a higher PV cell coverage ratio. Accordingly, this should also increase the temperature and reduce the conversion efficiency of the solar cells. In the present study, the temperature and conversion efficiency of solar cells were investigated throughout March 1 2013 (Fig. 5). The results demonstrate that conversion efficiency decreases with increasing temperature. At noon, the temperature for the 80% PV cell coverage ratio case was 7°C higher than that for the 10% PV cell coverage ratio case; this temperature difference corresponded to a 0.007 decrease in conversion efficiency, which was 5.5% lower than the 10% PV cell coverage ratio case. Thus, the results demonstrate the importance of considering PV cell coverage ratio in PV electricity generation.

3.2 Effects on lighting electricity consumption

The amount of daylight blocked by solar cells can vary considerably in response to differences in PV cell coverage ratio between semi-transparent PV panels, which can have a vital impact on indoor illuminance. If the indoor illuminance drops below a given threshold, artificial lighting is required to achieve a comfortable lighting environment and electricity must be consumed to achieve this. However, room depth and WWR may also affect the performance of semi-transparent PV panels at different PV cell coverage ratio. Thus, it is important to understand the relationship between PV cell coverage ratio and indoor illuminance for different combinations of room depth and WWR.

For larger room depth (i.e. deeper rooms), it is more difficult for daylight to reach deep inside the room. Thus, even for the same PV cell coverage ratio, daylight illuminance will tend to vary depending on room depth conditions. The results show that indoor illuminance decreases rapidly with increasing PV cell coverage ratio, with more pronounced decreases for smaller room depths. In general, shorter rooms (i.e. smaller room depth) experience much higher daylight illuminance than deep rooms (i.e. larger room depth). Moreover, indoor illuminance remains below 400 lux for all cases in which room depth exceeds 9 m. These results demonstrate that the effects of PV cell coverage ratio on daylight illuminance are strongly dependent on room depth.
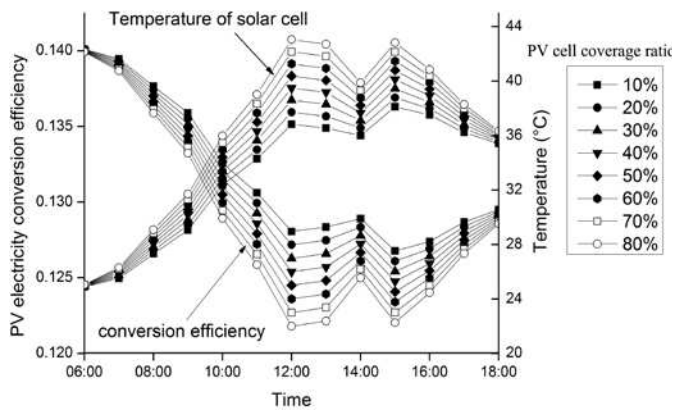
Fig. 5 Solar cell temperature and conversion efficiency for different PV cell coverage ratio
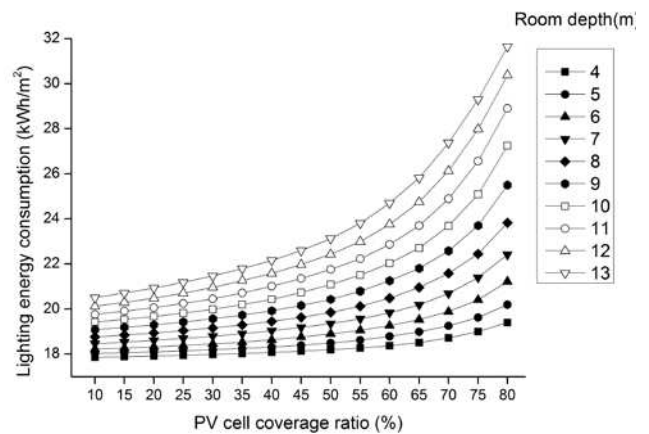
Fig. 6 Lighting electricity consumption for different PV cell coverage ratio for various room depth cases

Figure 6 illustrates the lighting electricity consumed for artificial lighting (which compensates for natural daylight) for different PV cell coverage ratio in different room depth cases. It is clear that this electricity consumption increases when daylight illuminance decreases in response to high PV cell coverage ratio. However, the relationship between consumption and PV cell coverage ratio is not linear. For small room depth, lighting electricity consumption increases much more rapidly when PV cell coverage ratio exceeds 50%; conversely, for larger room depth cases, the overall trend is much closer to a linear relationship. Cases in which room depth is small typically consume less lighting electricity (15 kWh/m^2 less at most) owing to their high indoor illuminance.

A greater WWR allows more daylight to penetrate into the room and presents a greater window area upon which semi-transparent PV panels can be installed.. However, the results show that the impact of WWR on daylight illuminance is less pronounced than that of room depth. A similar pattern is apparent in the results demonstrating the relationship between lighting electricity consumption and PV cell coverage ratio for variable WWR (Fig. 7): lighting electricity consumption increases with increasing PV cell coverage ratio, although the differences between different WWR cases are relatively small, with electricity savings of 9 kWh/m^2 at most (at 80% PV cell coverage ratio).

3.3 Effects on heating and cooling electricity consumption

Heating and cooling loads of office buildings are more easily affected by solar radiation, as office buildings typically function primarily during daytime. Varying the amount of solar radiation entering a building by installing semi-transparent PV panels with different PV cell coverage ratio can have an impact on heating and cooling loads. Increasing the influx of solar radiation can reduce heating demand in winter; however, it also increases cooling demand in summer. Figure 8 illustrates the heating and cooling electricity consumption for different PV cell coverage ratio for several room depth cases with a fixed WWR of 0.35. Heating and cooling electricity consumption first decreases with increasing PV cell coverage ratio, although the rate of decrease slows when PV cell coverage ratio exceeds 50%. The cases with higher PV cell coverage ratio appear to perform better in terms of heating and cooling energy savings based on annual data. This can be attributed

primarily to the climatic conditions in central China, where the cooling load in summer is typically greater than the heating load in winter. However, the benefits of high PV cell coverage ratio become less pronounced as room depth increases: the shortest room has the highest heating and cooling electricity consumption, although variations in consumption with changes in room depth become less pronounced when room depth exceeds 9 m. These results highlight the importance of considering PV cell coverage ratio, particularly in cases with small room depth.

Figure 9 illustrates the heating and cooling electricity consumption for different PV cell coverage ratio in cases with different WWR. As for the cases with variable room depth, heating and cooling electricity consumption first decreases with increasing PV cell coverage ratio, with the rate of decrease slowing when PV cell coverage ratio exceeds 60%. Cases with small WWR typically perform better in terms of heating and cooling energy saving, and the effects of varying PV cell coverage ratio are typically less pronounced when WWR is small. However, in such cases, the effects of WWR remain relatively constant between cases, meaning that heating and cooling electricity consumption will continue to increase with increasing WWR, with no signs of slowing down or stabilising.
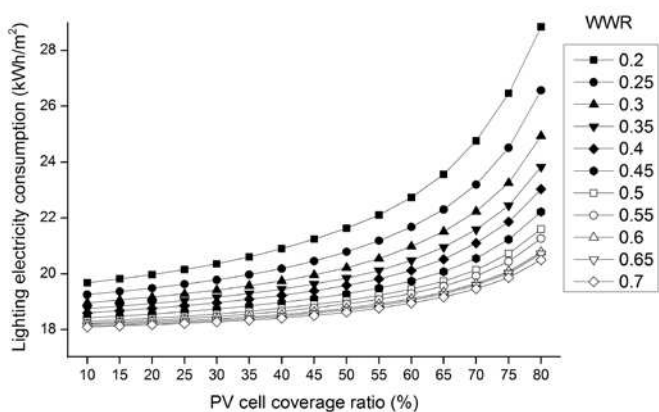

Fig. 7 Lighting electricity consumption for different PV cell coverage ratio for various WWR cases
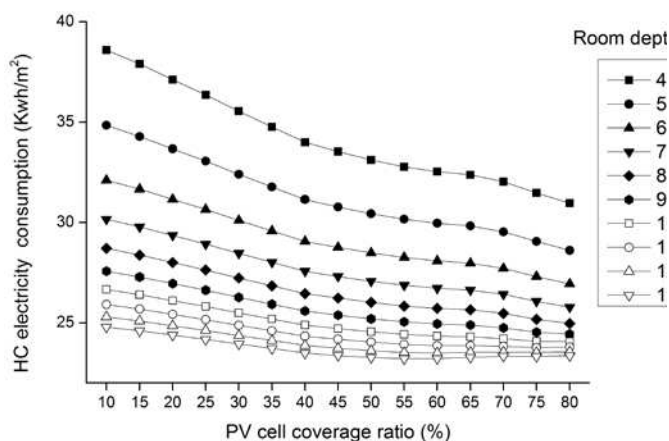

Fig. 8 Heating and cooling electricity consumption for different PV cell coverage ratio for various room depth cases
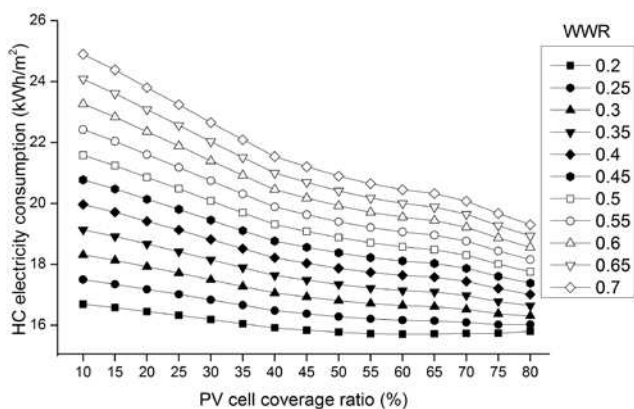

Fig. 9 Heating and cooling electricity consumption for different PV cell coverage ratio for various WWR cases

3.4 Effects on overall energy performance

Based on the analysis presented above, it can be concluded that increasing PV cell coverage ratio under the climatic conditions in central China typically leads to decreases in PV electricity conversion efficiency and heating and cooling electricity consumption, but increases in lighting electricity consumption. However, the effects of room depth and WWR on these relationships are pronounced, demonstrating that these factors must be considered carefully when designing semi-transparent PV technology for buildings. Therefore, it is necessary to evaluate overall energy consumption considering all of these factors to allow determination of an optimal PV cell coverage ratio. In such case, overall energy consumption is defined as following.

Overall energy consumption = Lighting energy consumption + cooling and heating energy consumption – PV electricity generation. Figures 10(a) and (b) illustrate the overall energy consumption for cases with large WWR (0.6) for two different values of room depth (6 m and 12 m, respectively). For a room depth of 6 m, PV cell coverage ratio of 80% achieves the lowest overall electricity consumption, allowing electricity savings of 18.9% compared to the case with PV cell coverage ratio of 10%. This can be attributed primarily to the influence of heating and cooling electricity consumption: high PV cell coverage ratio can reduce the enormous cooling demands for short rooms. Conversely, for a room depth of 12 m, the greatest electricity savings are achieved for PV cell coverage ratio of 50%. This can be attributed primarily to decreases in lighting electricity consumption during daytime owing to the smaller PV cell coverage ratio; these savings overwhelm the effects of heating and cooling electricity consumption.

Figures 11(a) and (b) illustrate the overall energy consumption for cases with small WWR (0.3) for two different values of room depth (6 m and 12 m, respectively). In such cases, PV electricity generation is typically very small compared to lighting and heating and cooling electricity consumption owing to the limited area available for the installation of semi-transparent PV panels. However, the influence of PV cell coverage ratio remains pronounced, particularly in terms of its effects on daylight and heating and cooling demand. For the 6 m room, PV cell coverage ratio of 60% achieves the lowest electricity consumption, with electricity savings of 6.8% compared to PV cell coverage ratio of 10%. Conversely, in the 12 m room, PV cell coverage ratio of 20% achieves the lowest electricity consumption, with electricity savings of 17.3% compared to PV cell coverage ratio of 80%.

3.5 Optimal PV cell coverage ratio

Based on the parametric analysis above, it is clear that an optimal PV cell coverage ratio (i.e. that which will achieve the lowest overall electricity consumption) can be obtained based on a particular combination of WWR, room depth, and orientation. Thus, optimal PV cell coverage ratio should be selected by comparing the overall energy consumption results for all PV cell coverage ratio cases under different architectural conditions (i.e. WWR, room depth, and orientation). The southern orientation is typically affected more extensively by solar energy than other orientations; accordingly, it is often the preferred orientation for the installation of photovoltaic applications. Variations in WWR and room depth can lead to considerable variation in optimal PV cell coverage ratio (Table 4).

Differences in electricity consumption between the most and least favourable PV cell coverage ratio were calculated; in particular, electricity savings for different combinations of room depth and WWR were calculated. The results demonstrate electricity savings ranging from 5% to 30%, with an average saving of 13% for the optimal PV cell coverage ratio. Moreover, optimal PV cell coverage ratio was found to be particularly

important in short rooms with large WWR, where electricity savings of over 20% were achieved.

Variations in optimal PV cell coverage ratio were also investigated. Optimal PV cell coverage ratio was found to decrease with increasing room depth (i.e. from 4 m to 13 m). This can be attributed primarily to the fact that the electricity demand during daytime increases faster than the compensation achieved through savings in heating and cooling. This also explains why rooms with greater depths typically have smaller optimal PV cell coverage ratio. Furthermore, optimal PV cell coverage ratio increases when WWR increases from 0.2 to 0.7, primarily because the electricity savings achieved by adopting a larger WWR (combined with the greater PV electricity generation and lower cooling load) result in higher optimal PV cell coverage ratio.

(a).

(b).

Fig. 10 Changes in overall energy consumption in response to variations in WWR and room depth: (a) room depth = 6 m, WWR = 0.3; (b) room depth = 12 m, WWR = 0.3;

(a).

(b).
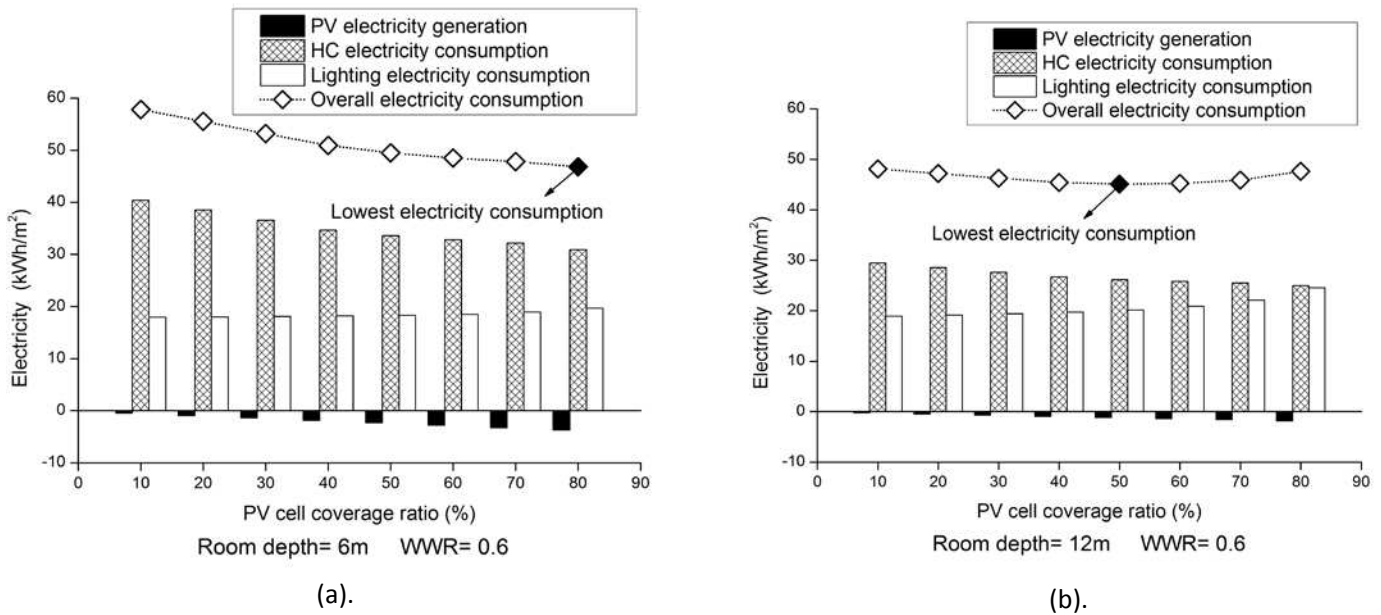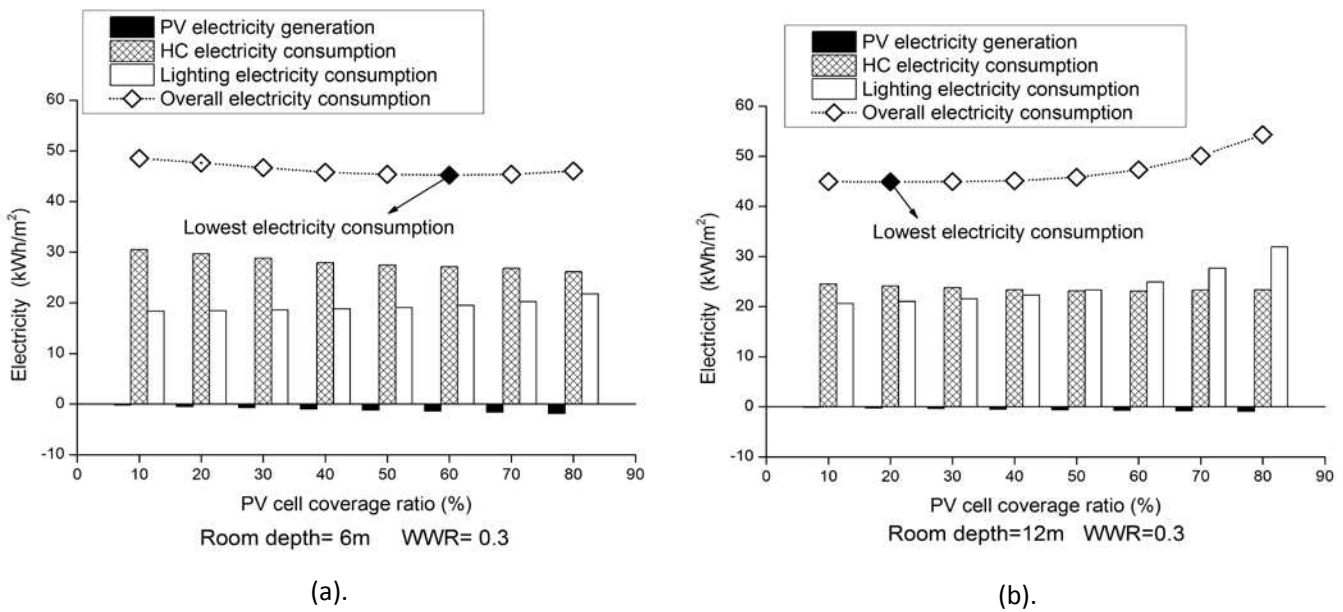
Fig.11 Changes in overall energy consumption in response to variations in WWR and room depth: (a) room depth = 6 m, WWR = 0.6; (b) room depth = 12 m, WWR = 0.6

Table 4 Optimal PV cell coverage ratio for different combinations of room depth and WWR in southern orientation

WWR	optimal PV cell coverage ratio (%) room depth (m)									
	4	5	6	7	8	9	10	11	12	13
0.2	75	55	50	40	35	20	10	10	10	10
0.25	80	60	55	50	40	40	30	10	10	10
0.3	80	75	60	55	50	40	40	30	20	10
0.35	80	80	75	55	55	45	40	40	35	30
0.4	80	80	75	60	55	50	45	40	40	40
0.45	80	80	80	75	60	55	50	45	40	40
0.5	80	80	80	75	70	60	55	50	45	40
0.55	80	80	80	80	75	60	55	55	50	45
0.6	80	80	80	80	75	75	60	55	55	50
0.65	80	80	80	80	75	75	60	60	55	50
0.7	80	80	80	80	80	75	75	60	55	55

To demonstrate the effects of different orientations on optimal PV cell coverage ratio, different combinations of orientation and room depth (WWR) were investigated with WWR (room depth) fixed at 0.35 (8 m); orientation was varied between east, southeast, south, southwest, and west (Tables 5 and 6). The northern orientation was not included in this investigation because it is known to be particularly unfavourable for PV applications. The results demonstrate that the optimal PV cell coverage ratio is highest in the west orientation. Under the climatic conditions prevalent in central China, cooling demands in summer typically exceed heating demands in winter. Thus, in summer, high PV cell coverage ratio can reduce the cooling load associated with the heat accumulated indoors during daytime.

Table 5 Optimal PV cell coverage ratio for different combinations of orientation and room depth

orientation	optimal PV cell coverage ratio (%) room depth (m)									
	4	5	6	7	8	9	10	11	12	13
E	75	60	50	45	35	25	20	20	20	15
SE	75	60	50	45	40	35	30	30	25	20
S	80	80	75	55	55	45	40	40	35	30
SW	80	80	75	65	55	50	50	45	40	35
W	80	80	80	75	65	55	55	50	45	40

Table 6 Optimal PV cell coverage ratio for different combinations of orientation and WWR

orientation	optimal PV cell coverage ratio (%)										
	WWR										
	0.2	0.25	0.3	0.35	0.4	0.45	0.5	0.6	0.6	0.65	0.7
E	25	40	40	45	50	60	60	60	70	70	70
SE	25	40	40	45	50	60	60	65	70	70	75
S	35	40	50	55	55	60	70	75	75	75	80
SW	35	50	50	60	65	65	70	75	75	75	80
W	35	50	50	60	65	65	70	75	75	75	80

4. Conclusions

In the present study, calculation models were established to investigate the properties of semi-transparent PV installations in relation to PV cell coverage ratio and the models were validated using data obtained in field experiments. In particular, an architectural model was developed to incorporate a series of generic office rooms. The validated calculation methods and properties were incorporated into Energy Plus to perform a parametric analysis of the effects of different PV cell coverage ratio on electricity consumption under different architectural conditions (room depth, WWR, and orientation). The results of the study can be summarised as follows.

(1) PV electricity conversion efficiency decreases as PV cell coverage ratio increases. Conversion efficiency decreases by 5.5% as PV cell coverage ratio is increased from 10% to 80%. (2) With increasing PV cell coverage ratio, indoor daylight illuminance decreases linearly and electricity consumption increases. Room depth appears to have a greater effect than WWR on both daylight illuminance and lighting electricity consumption. (3) Under the climatic conditions of central China, increasing PV cell coverage ratio appears to result in decreases in heating and cooling electricity consumption. (4) When overall energy performance is considered, adopting optimal PV cell coverage ratio can result in electricity savings of up to 30% (average savings: 13%) compared to the least favourable PV cell coverage ratio, although the savings achieved vary depending on the combination of room depth and WWR adopted, at least in the south orientation. This demonstrates the importance of selecting optimal PV cell coverage ratio based on architectural conditions. (5) In rooms with small room depth, optimal PV cell coverage ratios are relatively small compared to rooms with larger room depths. In rooms with large WWR, optimal PV cell coverage ratios are relatively large compared to rooms with small WWR. This means that PV façades with high PV cell coverage ratios are more suitable for deep rooms with larger windows, whereas the PV façades of small PV cell coverage ratio are more suitable for short rooms with small windows. (5) Building orientation can also affect the optimal ratio, with changes of 5–10% depending on specific orientation and optimal PV cell coverage ratio. Changes are typically highest in the western orientation; however, these changes induced by orientation are much less pronounced than those induced by variation in WWR and room depth.

It is hoped that the results presented here will act as a general reference point for the selection of optimal PV cell coverage ratio in the semi-transparent PV design approach. In particular, the present study should provide assistance in maximising the benefits of semi-transparent PV application with reference to the overall

energy performance of buildings, including electricity generation, lighting, and cooling and heating. Thus, these results represent a solid foundation for the optimisation of the architectural design of office buildings with semi-transparent PV façades.

References
[1] S. Natarajan, G.J. Levermore, Domestic futures—Which way to a low-carbon housing stock? Energy Policy 35(11) (2007) 5728-5736.
[2] S. Roberts, Building Integrated Photovoltaics, first ed., Birkhäuser Architecture, Berlin, 2009.
[3] B. Weller. Detail Practice: Photovoltaics: Technology, Architecture, Installation, Basel, 2010.
[4] X. Zhang, X. Zhao, S. Smith, J. Xu, X. Yu, Review of R&D progress and practical application of the solar photovoltaic/thermal (PV/T) technologies, Renewable and Sustainable Energy Reviews, 16(1) (2012) 599-617.
[5] H.M. Taleb, A.C. Pitts, The potential to exploit use of building-integrated photovoltaics in countries of the Gulf Cooperation Council, Renewable Energy, 34(4) (2009) 1092-1099.
[6] J.C. Lam, D.H.W. Li, S.O. Cheung, An analysis of electricity end-use in air-conditioned office buildings in Hong Kong, Building and Environment, 38(3) (2003) 493-498.
[7] C. Peng, Y. Huang, Z. Wu, Building-integrated photovoltaics (BIPV) in architectural design in China, Energy and Buildings, 43(12) (2011) 3592-3598.
[8] D.H.W. Li, T.N.T. Lam, W.W.H Chan, A.H.L. Mak, Energy and cost analysis of semi-transparent photovoltaic in office buildings, Applied Energy, 86(5) (2009) 722-729.
[9] T.Y.Y. Fung, H. Yang, Study on thermal performance of semi-transparent building-integrated photovoltaic glazings, Energy and Buildings, 40(3) (2008) 341-350.
[10] B. Jiang, J. Ji, H. Yi, The influence of PV coverage ratio on thermal and electrical performance of photovoltaic-Trombe wall, Renewable Energy, 33(11) (2008) 2491-2498.
[11] P.W. Wong, Y. Shimoda, M. Nonaka, M. Inoue, M. Mizuno, Semi-transparent PV: Thermal performance, power generation, daylight modelling and energy saving potential in a residential application, Renewable Energy, 33(5) (2008) 1024-1036.
[12] T. Miyazaki, A. Akisawa, T. Kashiwagi, Energy savings of office buildings by the use of semi-transparent solar cells for windows, Renewable Energy, 30(3) (2005) 281-304.
[13] G.Y. Yun, M. McEvoy, K. Steemers, Design and overall energy performance of a ventilated photovoltaic façade, Solar Energy, 81(3) (2007) 383-394.
[14] E.L. Didoné, A. Wagner, Semi-transparent PV windows: A study for office buildings in Brazil, Energy and Buildings, 67 (2013) 136-142.
[15] P.K. Ng, N. Mithraratne, H.W. Kua, Energy analysis of semi-transparent BIPV in Singapore buildings, Energy and Buildings, 66 (2013) 274-281.
[16] L. Lu, K.M. Law, Overall energy performance of semi-transparent single-glazed photovoltaic (PV) window for a typical office in Hong Kong, Renewable Energy, 49 (2013) 250-254.
[17] L. Olivieri, E. Caamaño-Martín, F. Olivieri, J. Neila, Integral energy performance characterization of semi-transparent photovoltaic elements for building integration under real operation conditions, Energy and Buildings, 68(Part A) (2014) 280-291.

[18] Z. Ye, A. Nobre, T. Reindl, J. Luther, C. Reise, On PV module temperatures in tropical regions, Solar Energy, 88 (2013) 80-87.

[19] E. Skoplaki, J.A. Palyvos, On the temperature dependence of photovoltaic module electrical performance: A review of efficiency/power correlations, Solar Energy, 83(5) (2009) 614-624.

[20] Ministry of Housing and Urban-Rural Development of the People's Republic of China, Calculation Specification for Thermal Performance of Windows, Doors and Glass Curtain-walls, China Architectural & Building Press, Beijing, 2008.

[21] China Academy of Building Research, Standard for Lighting Design of Buildings, China Architectural & Building Press, Beijing, 2008.

[22] China Academy of Building Research, Design Standard for Energy Efficiency of Public Buildings, China Architectural & Building Press, Beijing, 2004.